27

Effect of the Repulsive Interactions on the Nucleation and Island Growth: Kinetic Monte Carlo Simulations

Hu Juanmei and Wu Fengmin
Institute of Condensed Matter Physics, Zhejiang Normal University, Jinhua, Zhejiang 321004
People's Republic of China

1. Introduction

The initial stages of the thin-film epitaxy, such as nucleation and island growth, are important to the synthesis of a wide variety of interfacial materials. The island nucleation process is typically described by the mean-field nucleation theory (Venables J. A., 1973; Venables J. A. et al., 1984), which can be solved to predict the density of stable islands as a function of the deposition rate and the diffusivity of an isolated adatom at low temperatures, such as $Nx\sim(F/D)^{1/3}$. Its validity has been investigated experimentally in studies of several homo- and hetero-epitaxial growth systems (Brune H., 1998; Brune H. et al., 1999; Amar J. G. & Family F., 1995; Ratsch C. et al., 1994). However, both experiment and theory indicate that the nucleation theory is no longer valid when the adatom-adatom interactions beyond the nearest-neighbor sites are taken into account at low temperatures (Brune H. et al., 1995; Barth J.V. et al., 2000; Fischer B. et al., 1999; Bogicevic A.,et al., 2000).

The long-range interactions between adatoms on the noble metal surfaces have received considerable experimental and theoretical interest during the recent years (Torrente F. et al., 2007; Ziegler M. et al., 2008; Nanayakkara S. U. et al., 2007). The interactions have been explained by Friedel oscillations in the surface-state electrons, since they show the characteristic asymptotic dependence as $E(r)=-A\sin(2kFr+2\delta)/r^2$ (Lau K. H. et al., 1978). Low-temperature STM studies have resolved the long-range interactions mediated by surface states at large interatomic separations (Repp J. et al., 2000; Knorr N. et al., 2002) and found local diluted hexagonal structures. In addition, the long-range interactions are also considered as the driving force for the formation of the superlattice (Silly F. et al., 2004; Negulyaev N. N. et al., 2006). Several theoretical studies have demonstrated that those indirect interactions can highly affect atomic motion and the growth processes despite the fact that they are relatively small. For example, Bogicevic *et al.* (Bogicevic A. et al., 2000; Ovesson S. et al., 2002) revealed a large increase of island density when the long-range interactions are taken into account. Fichthorn *et al*. (Fichthorn K. A. & Scheffler M., 2000) found that the long-range interactions between Ag adatoms on a strained Ag(111) surface are comparable to the diffusion barrier, which can significantly influence the surface diffusion and the growth morphology in a thin-film epitaxy. Combine with kinetic Monte Carlo simulations, Fichthorn *et al.* (Fichthorn K. A. et al., 2002, 2003; Merrick M. L. et al.,

2003*)* also found that the repulsive interactions make the island densities over an order of magnitude larger than those predicted by nucleation theory. In addition, the repulsive part of interactions can lead to monodisperse islands early in the deposition process.

The effect of the long-range interactions on fabricating nanostructures are divided into two branches: the formation of uniformly distributed islands such as quantum dots (Liu C. H. et al., 2006; Negulyaev N. N. et al., 2008) and the large scale of superlattice which consists of regularly monomers in hexagonal structures or nanochains (Silly F. et al.; Ding H. F. et al., 2007; Negulyaev N. N. et al., 2008; Negulyaev N. N. et al., 2009).

In the present work, the nucleation and island growth on (111) surface in considering the repulsive interactions are systematically investigated by kinetic Monte Carlo (kMC) simulations. The dependence of radius, the attenuation rate, the intensity of the repulsive interactions and the diffusion barrier on the island density is discussed in detail. Based on the study, a relatively clear understanding of the relationship between the island density and repulsive interactions is obtained.

2. The kMC simulation model

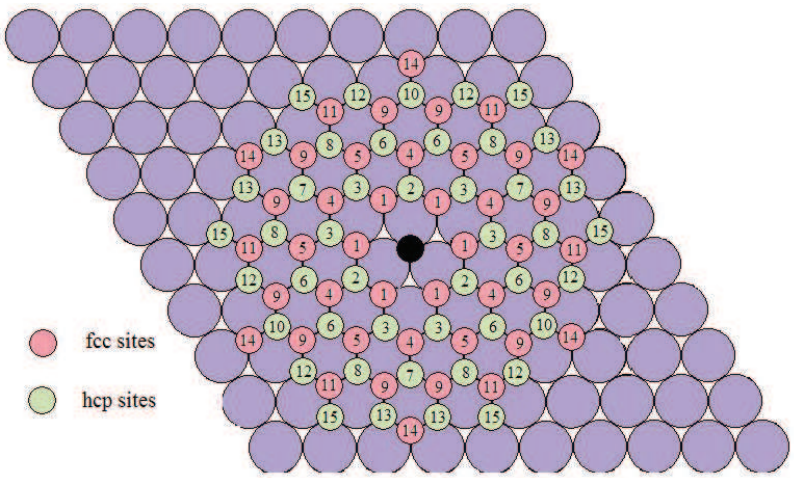

Fig. 1. Schematic illustration of the (111) substrate and possible adsorption sites. The big purple particles denote the (111) substrate. The black dot in the center denotes the position of one adatom on the substrate and other small dots indicate possible positions of a second adatom. The red dots represent fcc sites and the green dots represent the hcp sites. The number on the small dots indicates the ith neighbors from the central adatom.

As shown in Figure 1, the (111) substrate is represented as a triangular lattice with two non-equivalent adsorption sites (fcc and hcp) with a separation of $a_0 / \sqrt{3}$ between the nearest sites, where a_0 is the lattice constant of the substrate. Adatoms can only diffuse from the current fcc (hcp) site to one of the nearest empty hcp (fcc) sites at low temperature. The diffusion rate of an adatom from site k to site j on the (111) surface is calculated using the expression $v_{k\to j} = v_0 \exp(-E_{k\to j} / k_B T)$, where $v_0 = 10^{12}$ s^{-1} is the attempt frequency (Fichthorn K.A. et al., 2000), $E_{k\to j}$ is the barrier between site k and site j k_B is the Boltzmann constant.

The influence of the adatom-adatom interactions on diffusion is included in the barrier which takes the form: $E_{k\to j} = E_d + 0.5(E_j - E_k)$. Here, E_d is the diffusion barrier for an isolated atom on a clean surface, $E_{k(j)}$ is the sum of the pair interactions of the hopping adatom with all other adatoms in the system when the hopping adatom is at site $k(j)$. The difference of diffusion barriers between fcc and hcp sites and the effect of tri-adatoms interactions are neglected in our simulation. The simulation box is set to 200 a_0 x 200 a_0 with the periodic boundary conditions. The deposition rate is fixed at F=0.01ML/s during the simulation. Therefore, the step interval between two continuous depositions is $v_0\exp(-E_d/k_BT)/(200\text{x}200F)$. The simulation stops when the coverage reaches 0.05ML and there is no isolated adatoms.

The specific configuration of the (111) surface in figure 1 shows that the central adatom is surrounded alternately by fcc (red dots) and hcp (green dots) sites. The repulsive barriers we defined here is either at hcp sites or fcc sites. Thus the shape of the repulsive rings is hexagonal. The numbers on each small site in Figure 1 mean the ith neighbors from the central adatom. The interactions between more than two adatoms are described by pairwise summation (Österlund L.et al., 1999; Fichthorn K. A. et al., 2003).

3. Simulation results and discussion

3.1 The radius of the repulsive ring

Different species of adatom and substrate have different long-range interactions, including the intensity, the location of the repulsive barriers and the attenuation rate despite of the similar origin. The location of the repulsive barriers of Cu/Cu(111) is at 12 Å (9th-11th neighbors) (Repp J. et al., 2000) while that of Ag on strained Ag(111) is at about 10th-13th neighbors (Fichthorn K. A. et al., 2000). Thus the effect of the location of the repulsive barriers to the island density is necessary to be studied. As shown in figure 1, around the central adatoms, the possible locations are alternant between fcc sites and hcp sites. In this study, the location of the repulsive barriers are assumed to be at the 2-3th, 4-5th, 6-7-8th, 9-11th, 10-12-13-15th, and 14-16-18th neighbors, respectively. In all these cases, there is only one repulsive barrier with unique intensity before the formation of island. Thus, the range of the repulsive barriers is the same and only effect of the distance from the adatom to the repulsive barriers (the radius of the repulsive ring) is considered.

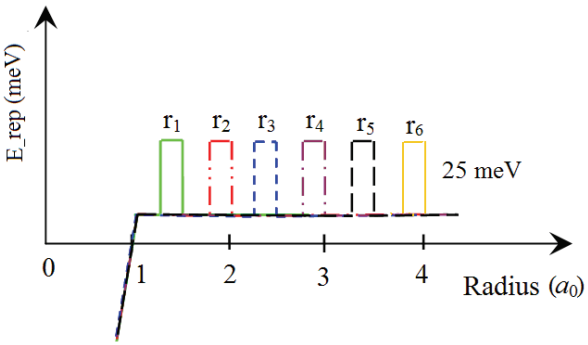

Fig. 2. Schematic illustration of the location of the repulsive barriers with unique intensity. a_0 is the lattice constant of the substrate. The intensity of the repulsive barriers is set to 25 meV.

The schematic illustration of the locations of the repulsive barriers is shown in Figure 2. The intensity of the repulsive barrier is 25 meV, which is the same as the diffusion barrier. The substrate temperature is set to 20 k. In Figure 3(a), we show the relationship between the island density and the location of the repulsive barriers. With the increase of the radius of the repulsive ring, the island density increase quickly at first then reach the saturation when the barrier is at about 12th neighbors and at last decrease with the continuous increasing distance.

In the simulation, the adatom-adatom interactions are pairwise and the barriers around the island are the summation of the interactions comes from all the atoms in the island. Thus, the barrier around the island is larger than that around the isolated adatom, which makes the nucleation easier than the growth of the island. In addition, the barrier around the island depends on the radius of the repulsive ring even the size of the island is the same. An example is given in Figure 4. It is the potential energy map around a linear trimer with the repulsive barriers at 4-5th and 9-11th neighbors, respectively. We can see that the range of the repulsive barrier at the end of the trimer in Figure 4(b) is larger than that in Figure 4(a), which means that the monomers that overcome the repulsive barriers in Figure 4(b) will have more probabilities to fall back before forming a stable bond with the existing island. Beside the range of the repulsive barrier around the islands, adatoms with large radius of repulsive ring have higher probabilities to jump out to keep isolated when entered the repulsive ring of other adatoms.

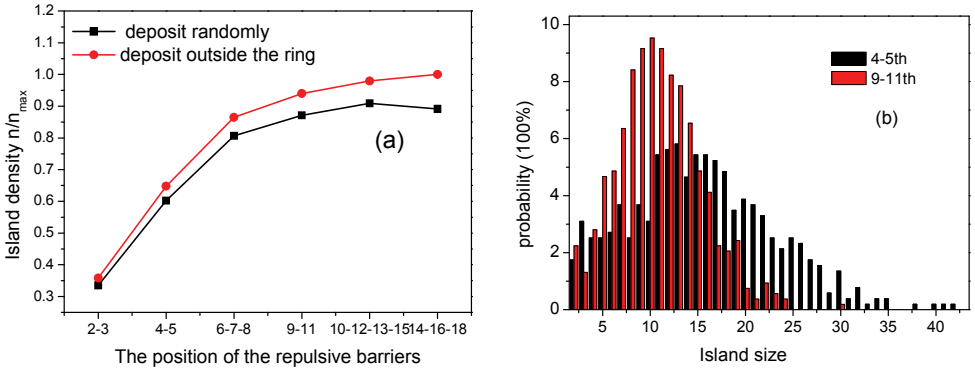

Fig. 3. (a) Island density as a function of the location of the repulsive barriers with randomly deposition and deposition only outside the repulsive ring. (b) Island size distribution with repulsive barriers at the 4-5th and 9-11th neighbors, respectively.

The decrease of the island density with the continuous increase of the radius comes from the deposition process. The probability to deposit inside the repulsive ring of other monomers or islands increases in square with the size of the repulsive ring. Spontaneously, the nucleation and growth occur easily when these events happen. To approve this, the atoms deposited inside the repulsive ring of other adatoms are cancelled until the distance between all of the adatoms and new adatom is larger than the repulsive ring. As shown the red curve in Figure 3(a), the island density not only increases monotonously until saturation but also has an up shift throughout the whole conditions studied.

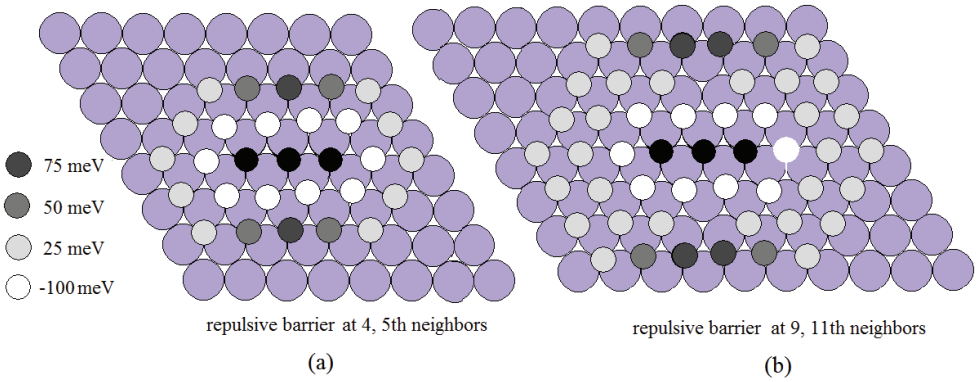

Fig. 4. Potential energy maps around a linear trimer with the location of the repulsive barriers at 4-5th neighbors and 9th-11th neighbors. The large purple particles represent the substrates, the three black dots in the center of the substrate represent the trimer. The gray dots in different colors mean different potential energy, the darker the larger of repulsive barriers.

Figure 3(b) is the results of the island size distribution with different radius of the repulsive ring. It shows that the distribution becomes sharper when the distance changes from 4-5th neighbors to about 9-11th neighbors. The average size of the island changes from 15 atoms to 11 atoms. This result implies that the position of the repulsive barriers is a candidate to modulate the size of the island to fabricate desired nanostructures.

3.2 The attenuation rate of the repulsive barriers

In the long-range interactions expression, another parameter varies in different materials is the attenuation rate of the repulsive ring. For example, the oscillation period on Cu(111) surface is about 15 Å(Repp J. et al., 2000) while on Ag(111) surface it is about 38 Å (Silly F. et al. 2004), which is more than twice longer than that of Cu. Thus the attenuation rate of the repulsive interactions is much small on the Ag(111) surface. In the previous case, we only investigated the radius of the repulsive ring with uniform attenuation rate (only one uniform barrier). In this part we will investigate the effect of the attenuation rate of the repulsive barriers on the island density. Due to the pairwise summation, it is too high for adatom to penetrate if high repulsive barrier is considered with small attenuation rate. So the largest repulsive barrier in this simulation is set to 4 meV at 4-5th neighbors.

The schematic illustration of the repulsive barriers with different attenuation rate is shown in Figure 5. The repulsive barriers decrease uniformly with the increase of radius by keeping the inner intensity fixed. Five different attenuation rates are studied and the results are shown in Figure 6. It can be seen that the island density is highly influenced by the attenuation rate of the repulsive barriers. The island numbers is more than 2 times larger when 5 attenuation rings are introduced instead of a single barrier with the same largest intensity. Based on the simulation model, the probability for one adatom to nucleate with another monomer is the same whether there is one large barrier or five small barriers if the largest barrier is fixed. The difference comes from the barriers around small islands. For example, in the five repulsive barriers condition, the potential energy at the end of the linear trimer in figure 4 is no longer uniform. It has grades and the largest barrier will have a climb

on the basis of uniform repulsive interaction, which makes the adatoms difficult to incorporate into the existing island. Therefore, the wavelength of the electronic gas on the metal surface is an important parameter affecting the growth of the island after nucleation.

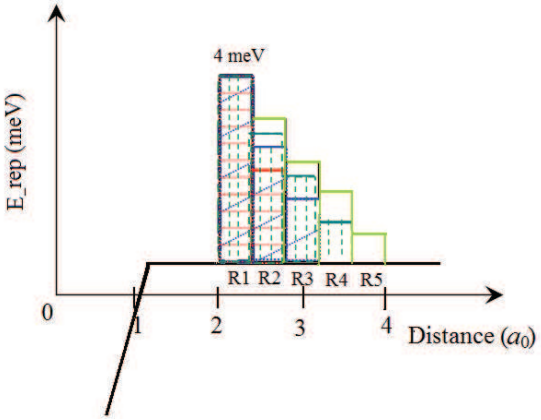

Fig. 5. Schematic illustration of repulsive barriers with different attenuation rate.

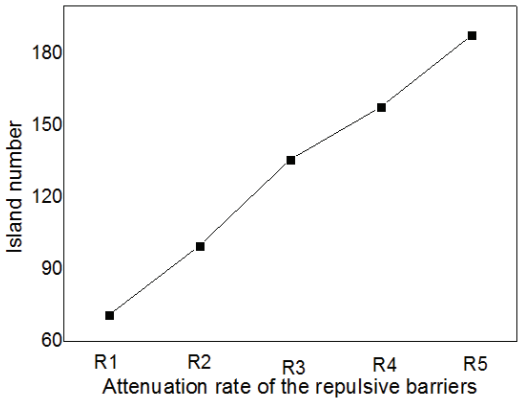

Fig. 6. The relation between the island density and the attenuation rate of the repulsive barriers.

3.3 The intensity of the repulsive rings

As Bogicevic *et al.* (Bogicevic A. et al., 2000; Ovesson S. et al., 2001) have already reported that there is a large increase of island density when the long-range interactions are taken into account. The increase of the island density originates from the repulsive part of long-range interactions around the adatoms which prevent the nucleation and the growth of the island. Here the specific effect of the intensity of the repulsive barrier on the island density is studied by fixing the diffusion barrier (25meV) and the location of the repulsive barrier (6-7-8th neighbors). The sketch map of the different repulsive barriers is given in figure 7. The intensities of repulsive barriers used are from 0 to 40 meV with an interval of 5 meV.

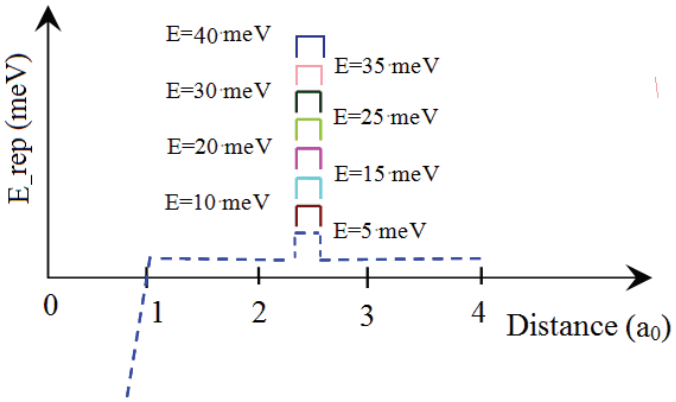

Fig. 7. Schematic illustration of the repulsive barriers around adatoms with the intensities from 0 to 40 meV. All of the locations of the barriers are at 6-7-8th neighbors.

According to the simulation model mentioned above, the influence of the adatom-adatom interaction on diffusion is included in the barrier taking the form: $E_{k\to j} = E_d + 0.5(E_j - E_k)$. So the probability to overcome the repulsive barrier of an monomer is as small as $0.5\exp(-E_{rep}/k_BT)$. Figure 8 shows the simulation results of the island density with different repulsive barriers. We can see that the island density increase sharply at small repulsive barriers. The number of islands increases from about 52 to 100 when only a 5meV barrier is taken into account.

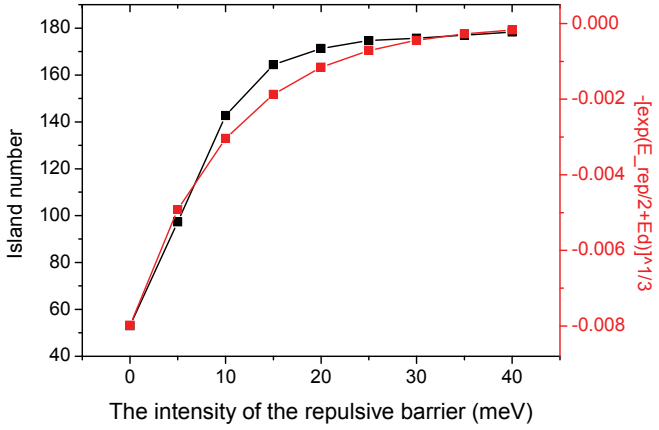

Fig. 8. The relation between the island density and the intensity of the repulsive barrier.

The increase rate of the island in figure 8 is compared with the expression $-[\exp(-E_{rep}/2-E_d)/k_BT]^{1/3}$, which satisfies the mean-field theory if the $E_{rep}/2+E_d$ is regarded as the diffusion barrier. We find that the increase rate of the island density is nearly comparable to the exiting theory when the repulsive barrier is small. Thus the effect of the repulsive barrier can be roughly treated as an increase of the diffusion barrier when the repulsive barrier is small at low temperature and low coverage.

3.4 The diffusion barrier

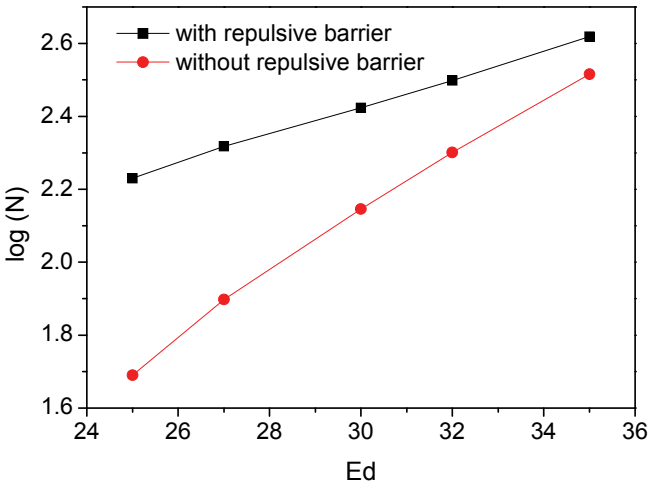

Fig. 9. Island density as a function of the diffusion barrier.

The diffusion barrier is another important parameter for the nucleation. The larger the diffusion barrier, the higher the temperature required for adatoms to diffuse and overcome the repulsive rings. In this part, the effect of the diffusion barrier on the nucleation is discussed after considering the repulsive barriers between adatoms. The results are given in figure 9. From the comparison whether considering the repulsive interactions or not, we find that both island densities are exponentially proportional the diffusion barrier. The difference is the slop of the line which decreases to one half when the repulsive barriers are considered. It means that the dependence of the island density on the diffusion barriers is no longer as sensitive as before. This result will be favored in heterogeneous growth where the diffusion barriers on the thin film are larger than that on the substrate.

4. Conclusions

Using kinetic Monte Carlo simulation, the effect of the repulsive part of the long-range interactions on the nucleation and island growth during thin film epitaxy is investigated. The parameters, including the radius, the attenuation rate, the intensity of the repulsive interactions, and the diffusion barrier of the substrate are discussed systematically. We find that the repulsive adatom-adatom interactions lead to higher island density than those without the repulsive interactions. The radius of the repulsive ring is an important factor determining not only the island density, but also the island size distribution. The slow attenuation repulsive rings can effectively block the growth of the existing islands. In addition, the island density depends sensitively on the intensity of repulsive barrier. Only a small repulsive interaction will highly increase the island density. Contrarily, the diffusion barrier is not as sensitive as that without repulsive interactions. The nucleation and growth mechanism which takes into account the repulsive interactions is propitious to layer-by-layer growth during the molecular beam epitaxy.

5. References

Amar J. G. & Family F. 1995 Critical Cluster Size: Island Morphology and Size Distribution in Submonolayer Epitaxial Growth. *Physical Review Letters* 74, 2066-2069.

Barth J.V., Brune H., Fischer B., Weckesser J. & Kern K. 2000. Dynamics of Surface Migration in the Weak Corrugation Regime. *Physical Review Letters* 84, 1732-1735.

Bogicevic A., Ovesson S., Hyldgaard P., Lundqvist B. I., Brune H. & Jennison D. R. 2000. Nature, Strength, and Consequences of Indirect Adsorbate Interactions on Metals. *Physical Review Letters* 85, 1910-1913.

Brune, H., 1998. Microscopic view of epitaxial metal growth: nucleation and aggregation. *Surf. Sci. Rep.* 31, 121.

Brune H., Bales G.S., Jacobsen J., Boragno C. & Kern K. 1991. Measuring surface diffusion from nucleation island densities. *Physical Review B,* 60, 5991-6006.

Brune H., Bromann K., Röder H., Kern K. 1995. Effect of strain on surface diffusion and nucleation. *Physical Review B, 52*, R14380-R14383.

Ding H. F., Stepanyuk V. S., Ignatiev P. A., Negulyaev N. N., Niebergall L., Wasniowska M., Gao C. L., Bruno P. & Kirschner J. 2007. Self-organized long-period adatom strings on stepped metal surfaces: Scanning tunneling microscopy, ab initio calculations, and kinetic Monte Carlo simulations. *Physical. Review B,* 76, 033409.

Fichthorn K.A., Scheffler M., 2000. Island Nucleation in Thin-Film Epitaxy: A First-Principles Investigation. *Physical Review Letters* 84, 5371-5374.

Fichthorn K. A., Merrick M. L. & Scheffler M., 2002. A kinetic Monte Carlo investigation of island nucleation and growth in thin-film epitaxy in the presence of substrate-mediated interactions. *Applied Physics A,* 75, 17-23.

Fichthorn K. A., Merrick M. L., 2003. Nanostructures at surfaces from substrate-mediated interactions. *Physical Review B,* 68, 041404(R).

Fischer B., Brune H., Barth J.V., Fricke A. & Kern K., 1999. Nucleation Kinetics on Inhomogeneous Substrates: Al/Au(111). *Physical Review Letters* 82, 1732-1735.

Knorr N., Brune H., Epple M., Hirstein A., Schnieder M. A. & Kern K., 2002. Long-range adsorbate interactions mediated by a two-dimensional electron gas. *Physical Review B,* 65, 115420.

Lau K. H. & Kohn W. 1978. Indirect long-range oscillatory interaction between adsorbed atoms. *Surface Science,* 75, 69-85.

Liu C. H., Matsuda I., D'angelo M., Hasegawa S. J., Okabayashi J., Toyoda S. & Oshima M., 2006. Self-assembly of two-dimensional nanoclusters observed with STM: From surface molecules to surface superstructure. *Physical Review B,* 74, 235420.

Merrick M. L., Luo W. W. & Fichthorn K. A., 2003. Substrate-mediated interactions on solid surfaces theory, experiment, and consequences for thin-film morphology. *Progress in Surface Science,* 72, 117-134.

Nanayakkara S. U., Sykes E. C. H., Torres L. C. F., Blake M. M. & Weiss P. S., 2007. Long-Range Electronic Interactions at a High Temperature: Bromine Adatom Islands on Cu(111). *Physical Review Letters* 98, 206108.

Negulyaev N. N., Stepanyuk V. S., Niebergall L., Hergert W., Fangohr H. & Bruno P., 2006. Self-organization of Ce adatoms on Ag(111): A kinetic Monte Carlo study. *Physical Review B,* 74, 035421.

Negulyaev N. N., Stepanyuk V. S., Hergert W., Bruno P. & Kirschner J., 2008. Atomic-scale self-organization of Fe nanostripes on stepped Cu(111) surfaces: Molecular dynamics and kinetic Monte Carlo simulations. *Physical Review B,* 77, 085430.

Negulyaev N. N., Stepanyuk V. S., Bruno P., Diekhöner L., Wahl P. & Kern K., 2008. Bilayer growth of nanoscale Co islands on Cu(111). *Phys. Rev. B* 77, 125437.

Negulyaev N. N., Stepanyuk V. S., Niebergall L., Bruno P., Pivetta M., Ternes M., Patthey F. & Schneider W-D., 2009. Melting of Two-Dimensional Adatom Superlattices Stabilized by Long-Range Electronic Interactions. *Physical Review Letters* 102, 246102.

Österlund L., Pedersen M. Ø., Stensgaard I., Lægsgaard E. & Besenbacher F. 1999. Quantitative Determination of Adsorbate-Adsorbate Interactions. *Physical Review Letters,* 83, 4812-4815.

Ovesson S., Bogicevic A., Wanhnström G. & Lundqvist B. I., 2001. Neglected adsorbate interactions behind diffusion prefactor anomalies on metals. *Physical Review B,* 64, 125423.

Ratsch C., Zangwill A., Smilauer P. & Vvedensky D. D., 1994. Saturation and scaling of epitaxial island densities. *Physical Review Letters,* 72, 3194-3197.

Repp J., Moresco F., Meyer G., Rieder K.-H., Hyldgaard P. & Persson M., 2000. Substrate Mediated Long-Range Oscillatory Interaction between Adatoms: Cu /Cu(111). *Physical Review Letters,* 85, 2981-2984.

Silly F., Pivetta M., Ternes M., Patthey F., Pelz J. P. & Schneider W. D., 2004. Coverage-dependent self-organization: from individual adatoms to adatom superlattices. *New Journal of Physics,* 6, 16.

Silly F., Pivetta M., Ternes M., Patthey F., Pelz J. P. & Schneider W. D., 2004. Creation of an Atomic Superlattice by Immersing Metallic Adatoms in a Two-Dimensional Electron Sea. *Physical Review Letters,* 92, 016101.

Torrente F., Monturet S., Franke K. J., Fraxedas J., Lorente N. & Pascual J. I., 2007. Long-Range Repulsive Interaction between Molecules on a Metal Surface Induced by Charge Transfer. *Physical Review Letters,* 99, 176103.

Venables J. A., 1973. Rate equation approaches to thin film nucleation kinetics. *Philosophycal Magazine,* 27, 697-738.

Venables J. A., Spiller G. D. T. & Hanbücken M., 1984. Nucleation and growth of thin films. *Reports on Progress Physics,* 47, 399.

Ziegler M., Kröger J., Berndt R., Filinov A. & Bonitz M., 2008. Scanning tunneling microscopy and kinetic Monte Carlo investigation of cesium superlattices on Ag(111). *Physical Review B,* 78, 245427.

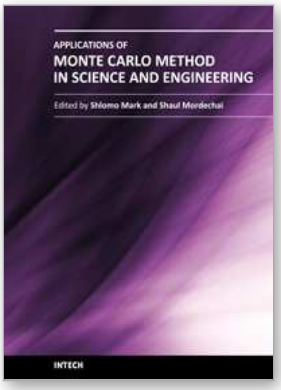

Applications of Monte Carlo Method in Science and Engineering
Edited by Prof. Shaul Mordechai

ISBN 978-953-307-691-1
Hard cover, 950 pages
Publisher InTech
Published online 28, February, 2011
Published in print edition February, 2011

In this book, Applications of Monte Carlo Method in Science and Engineering, we further expose the broad range of applications of Monte Carlo simulation in the fields of Quantum Physics, Statistical Physics, Reliability, Medical Physics, Polycrystalline Materials, Ising Model, Chemistry, Agriculture, Food Processing, X-ray Imaging, Electron Dynamics in Doped Semiconductors, Metallurgy, Remote Sensing and much more diverse topics. The book chapters included in this volume clearly reflect the current scientific importance of Monte Carlo techniques in various fields of research.

InTech Europe
University Campus STeP Ri
Slavka Krautzeka 83/A
51000 Rijeka, Croatia
Phone: +385 (51) 770 447
Fax: +385 (51) 686 166
www.intechopen.com

InTech China
Unit 405, Office Block, Hotel Equatorial Shanghai
No.65, Yan An Road (West), Shanghai, 200040, China
中国上海市延安西路65号上海国际贵都大饭店办公楼405单元
Phone: +86-21-62489820
Fax: +86-21-62489821